Reinforced Demand Side Management for Educational Institution with Incorporation of User's Comfort

Karthick Tamilarasu [1], Charles Raja Sathiasamuel [1,*], Jeslin Drusila Nesamalar Joseph [2], Rajvikram Madurai Elavarasan [3] and **Lucian Mihet-Popa [4,*]**

[1] Department of EEE, Thiagarajar College of Engineering, Madurai 625015, Tamil Nadu, India; karthi.ieee@gmail.com
[2] Department of EEE, Kamaraj College of Engineering and Technology, Madurai 625015, Tamil Nadu, India; jeslineee@kamarajengg.edu.in
[3] Clean and Resilient Energy Systems (CARES) Laboratory, Texas A&M University, Galveston, TX 77553, USA; rajvikram787@gmail.com
[4] Faculty of Electrical Engineering, Ostfold University College, 1757 Halden, Norway
* Correspondence: charlesrajas@tce.edu (C.R.S.); lucian.mihet@hiof.no (L.M.-P.)

Abstract: Soaring energy demand and the establishment of various trends in the energy market have paved the way for developing demand-side management (DSM) from the consumer side. This paper proposes a reinforced DSM (RDSM) approach that uses an enhanced binary gray wolf optimization algorithm (EBGWO) that benefits the consumer premises with load scheduling, and peak demand reduction. To date, DSM research has been carried out for residential, commercial and industrial loads, whereas DSM approaches for educational loads have been less studied. The institution load also consumes much utility energy during peak hours, making institutional consumers pay a high amount of cost for energy consumption during peak hours. The proposed objective is to reduce the total electricity cost and to improve the operating efficiency of the entire load profile at an educational institution. The proposed architecture integrates the solar PV (SPV) generation that supplies the user-comfort loads during peak operating hours. User comfort is determined with a metric termed the user comfort index (UCI). The novelty of the proposed work is highlighted by modeling a separate class of loads for temperature-controlled air conditioners (AC), supplying the user comfort loads from SPV generation and determining user comfort with percentage UCI. The improved transfer function used in the proposed EBGWO algorithm performs faster in optimizing nonlinear objective problems. The electricity price in the peak hours is high compared to the off-peak hours. The proposed EBGWO algorithm shift and schedules the loads from the peak hours to off-peak hours, and incorporating SPV in satisfying the user comfort loads aids in reducing the power consumption from the utility during peak hours. Thus, the proposed EBGWO algorithm greatly helps the consumer side decrease the peak-to-average ratio (PAR), improve user comfort significantly, reduce the peak demand, and save the institution's electricity cost by USD 653.046.

Keywords: smart grid; institutional loads; reinforced demand-side management; load-shifting; user comfort index; enhanced binary gray wolf optimization

1. Introduction

Demand-side management (DSM) is a very promising approach in a smart grid environment to minimize the energy consumption for the consumer and minimize the energy generation for the utility. The DSM algorithms and schemes include energy conservation programs, energy efficiency programs, and demand response (DR) programs. In the literature, there are different methods in which DSM has been implemented. Different types of the load management system have been implemented, such as a scheduling mechanism for interruptible loads over 16 h [1], a load-shifting based DSM controller for different categories of load in a residential area, commercial area, and industrial area [2],

a day-ahead load scheduler with user preference data has been developed for different classes of loads [3], a load-shifting based scheduler for the privacy protection of user energy consumption behavior [4], and a scheduler for controllable residential loads [5]. Different DSM schemes have been proposed for residential consumers, such as an intelligent residential energy management system (IREMS) [6], an optimization model for the operation of a residential microgrid in the presence of various distributed energy sources [7], and a real-time pricing scheme and progressive pricing scheme for smart grid system involving renewable energy resources [8].

The major objectives of DSM include minimization of the cost of energy consumption [1,3–6,8], reduction of peak demand [3,8], minimization of user dissatisfaction [1,4,5,8], and reduction of peak-to-average ratio PAR [3]. Minimizing the total annual cost of microgrids and total annual emission was acheived in [7]. In addition, the reduction in the distance between the actual load consumption curve and the optimized load consumption curve has been described in [2]. The major constraints handled are the maximum power demand limit [6], operational constraints of the loads, dynamics of renewable energy resources [6,8], battery constraints, and economic constraints.

A robust nonlinear controller used for a stand-alone DC microgrid with a battery, a photovoltaic panel (PV), and a supercapacitor [9] and the power flow through the tie-line is typically regulated at a prescheduled value, thereby enforcing the individual microgrid to manage their respective load at steady-state [10]. Theoretical graph analysis is presented to analyze per unit load sharing among all the nodes. The stability of the proposed controller is analyzed considering multiple source nodes using Lyapunov's approach [11]. Some of the load scheduling mechanisms in residential buildings have been reviewed. An intelligent universal load management scheduler (IULMS) can handle different power loads for a real-time residential apartment in India [12]. Exploring the possible demand response and load reduction opportunities under the smart grid for residential electricity load profile [13]. In [14], an intelligent residential load management system (IRLMS) can handle the dynamics of different types of residential loads.

Some of the research work has been focused on the scheduling of specific appliances. A load manager for scheduling the charging duration for electric vehicles (EV) and air-conditioners (AC) has been proposed in [15]. A stochastically formulated methodology used for modeling and analyzing the load demand in a domestic distribution system [16]. Distributed DSM systems were implemented based on the artificial immune network algorithm for air conditioning devices to meet the desired demand to tackle the peak load problem [17]. The effect of installing renewable energy sources also has been studied. The impact of wind energy penetration in the scheduling of reserves and energy in a smart distribution system was studied in [18]. A two-stage optimal scheduler was formulated for distributed generation sources in [19]. Demand response potential and characteristics of smart buildings load play a pivotal role in DR programs [20].

The role of educational buildings towards energy consumption across the world also has attracted researchers, and it is being explored. Long short-term memory (LSTM) based energy consumption forecasting model has been formulated in an academic building at IIT Bombay, India [21]. The institutional lab instruments are effectively managed to save energy and estimating the energy efficiency of educational loads [22]. The relation between using energy and space has been investigated for an educational building in Australia using multiple linear regression models in [23]. The optimal design and economical aspects of grid-interactive PV system configuration for an educational campus have been carried out using hybrid optimization of multiple electric renewable (HOMER) software [24]. The load pattern of energy consumption has been studied for Motilal Nehru national institute of technology (MNNIT), Allahabad, India, using a bottom-up load model [25]. Artificial intelligence techniques are also proposed to solve the energy demand planning in smart homes [26]. The dynamic performance of the energy management schemes is compared based on demand response programs [27]. Demand-side management is used with the PV and the thermal energy storage for peak electric load- shifting [28]. In general, the reach of

meta-heuristics algorithms is wide in computer scientists and researchers of other fields. The simplicity, flexibility, derivation-free mechanism, and local optimum avoidance made meta-heuristic algorithms more popular. The proposed RDSM technique deploys a GWO, enhancing its transfer function [29]. A game theory-based decentralized control strategy and a game theory-based fuzzy are developed to address the demand-side management problems [30]. Binary Gray Wolf Optimization [31] and Improved Binary Grey Wolf Optimization [32] approaches are used for solving non-linear problems. A demand-side management approach with user satisfaction is implemented for an institutional building [33]. An approach for cost optimization and is capable of giving maximum satisfaction to the user based on the predetermined user budget for an institutional building [34]. A coordinated load scheduling and controlling algorithm have been used to schedule the controllable appliances to minimize the peak load consumption [35]. A virtual queue stability-based Lyapunov optimization technique is employed for real-time energy and comfort optimization in grid-connected solar integrated smart buildings [36]. An innovative home appliance scheduling (IHAS) framework is proposed based on the fusion of the gray wolf and crow search optimization (GWCSO) algorithm to the cost of electricity reduction and user-comfort maximization [37]. A combinatorial heuristic-based profound-search algorithm (CHPSA) has been proposed for solving transmission expansion planning (TEP) problems in electric power networks considering wind power penetration [38]. Optimal power flow (OPF) is an important tool in the planning and operation of the power systems and aims to optimize the operational costs. The proposed fuzzy adaptive hybrid configuration oriented to a joint self-adaptive particle swarm optimization (SPSO) and differential evolution (FAHSPSO-DE) algorithms is very effective and robust for solving the OPF problem [39].

To date, from the literature review conducted, there are different methods of implementing DSM in DC microgrids, residential buildings, educational buildings, specific loads, and scheduling the various generation sources. Most of the previous DSM approaches were carried on residential, commercial and industrial loads, whereas DSM approaches for educational loads are less.

The RDSM technique is proposed to achieve the following objectives for the institution:

- Minimize the electricity consumption cost;
- Modeling a separate class of loads for air conditioners (AC);
- Significant reduction in PAR and peak demand;
- Shifts and schedules the institutional loads optimally by considering the constraints;
- User comfort index (UCI) is introduced that helps in increasing the user's satisfaction level for certain non-critical loads by incorporating the SPV.

The paper is organized as follows: Section 2 provides the proposed architecture of the RDSM–EBGWO algorithm. Section 3 presents the mathematical representation of the different classifications of load. Section 4 provides the problem formulation, objective function and constraints. Section 5 provides the details of the optimization algorithm. Section 6 provides implementing the proposed methodology with institutional user input data. Section 7 provides the results and discussion of the different cases. Section 8 presents the conclusion of the paper and enlightens on possible directions for future research.

Novelty

The DSM techniques for scheduling the loads are more common and popular in residential, industrial and commercial sectors. Educational institutions need DSM strategies to curtail their energy consumption significantly so that annual electricity costs are minimized. The RDSM is proposed for the educational institution Kamaraj College of Engineering and Technology (KCET), Tamil Nadu, India.

- The proposed reinforced demand-side management–enhanced binary gray wolf optimization (RDSM–EBGWO) approach shifts and schedules KCET institutional load optimally, accomplishing the main objective of minimizing the electricity consumption cost.

- Proposed a dedicated class for temperature-controlled loads, i.e., the air conditioner is modeled using the proposed RDSM–EBGWO, as this type of load contributes 80% of overall peak demand.
- Formulation of an index termed as user comfort index (UCI) to measure the degree of user's comfort before and after deployment of the proposed RDSM–EBGWO control.
- A 30 kW solar PV at the institutional premises is integrated into the UCI to increase the percentage of UCI. This lowers the energy consumption from the utility minimizing the electricity consumption cost.
- Performance comparison using metrics, such as peak-to-average ratio (PAR), reduction in peak demand and the cost savings was analyzed with binary particle swarm optimization (BPSO), binary gray wolf optimization (BGWO) and enhanced binary gray wolf optimization (EBGWO) algorithms.

2. Architecture

2.1. Proposed Architecture of RDSM–EBGWO

The main objective of the proposed RDSM–EBGWO is to curtail the total electricity cost by shifting and scheduling the institutional loads. The RDSM–EBGWO controller also helps in the improvisation of the institutional load consumption profile and UCI. To accomplish the objectives mentioned above, the load profile of KCET is studied and is categorized into four classes, namely uncontrollable non-shiftable loads (UNSLs), controllable Non-shiftable loads (CNSLs), uncontrollable shiftable loads (USLs), and controllable shiftable loads (CSLs).

UNSLs are loads that are fully uncontrollable and left for the user's choice. The UNSLs loads are a fan, lights, chargers, elevators, and local area network (LAN) communication, which are also called critical loads. The details, such as power consumption, period of operation, start and end time of the loads, are fetched from a separate UNSLs status collector. The architecture monitors whether the power consumption simultaneously exceeds the maximum demand limit (MDL). If the UNSLs loads exceed the MDL limit, a warning message is given to the particular load type.

Temperature-dependent loads such as air conditioners (ACs), water heaters, space heaters, geysers, etc., are classified under CNSLs. In this paper, only cooling loads are modeled, as cooling loads contribute to 95% of the temperature-dependent loads in KCET. The proposed RDSM–EBGWO controller has a dedicated status collector to monitor and log the parameters of ACs. The parameters collected by the CNSL status collector, such as setpoint temperature, the actual temperature at the instant of operation, tolerance limit, and AC cycle time, are shown in Figure 1. With these values, the RDSM–EBGWO controller shifts and schedules the operation of ACs optimally. The cycle time of AC is the number of times the AC switches ON/OFF within an hour of operation. An ideal AC, on average, has its cycle time as 4, i.e., AC switches ON/OFF every 15 min for an hour. The normal cycle time for the proper functioning of an AC on average is 4 times in an hour. When this cycle time is either increased or decreased, the efficiency of the AC diminishes or the AC malfunctions. The status collector sends a warning message to the RDSM–EBGWO controller whenever the cycle time of AC exceeds the limit.

The tolerance limit of AC is affected by the following:

- Ambient temperature;
- Human ambulation;
- Climate, weather, and season;
- Cycle time.

These factors affect the tolerance limit cycle time of AC and play a major role in scheduling the AC. The cycle time affects the power consumption of AC to an ample level. Figure 1 is a pictorial representation of the parameters and factors involved in the modeling of class 2.
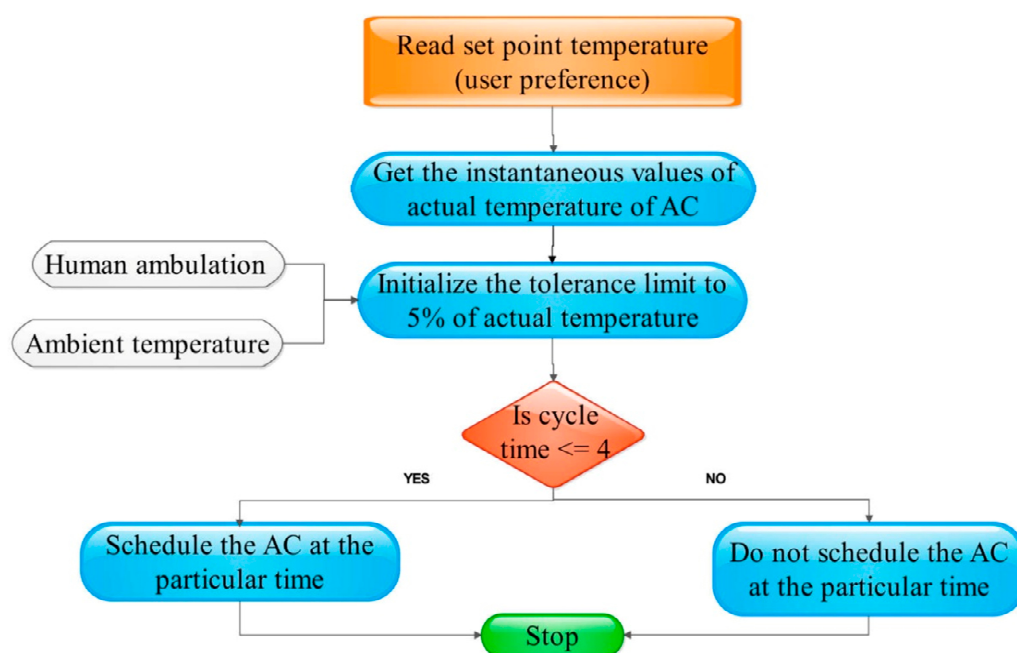
Figure 1. Modeling of CNSL.

The loads that can be controlled, shifted, and operated either continuously or discontinuously within its period of operation are categorized as shiftable loads (SLs). The shiftable loads are further classified as continuously operating uncontrollable shiftable loads (USLs) and discontinuously operating controllable shiftable loads (CSLs). Devices like inverters, batteries are categorized in USLs, which can be scheduled but cannot be interrupted during its period of operation. Laboratory loads, Plug-in hybrid vehicles, Pumps, compressors, etc., are modeled under CSLs that can be interrupted during its period of operation. The USL and CSL have separate status collectors that collect the status of the device and enlist them in their respective categories.

Figure 2 depicts the architecture of the proposed RDSM–EBGWO that has a separate control for each category of load types classified. The smart meters installed at the institutional premises collect the values of the parameters like the demand of the devices, instantaneous power drawn from the utility, etc. These values are logged in some data loggers to store and retrieve data as and when it is needed. With the parameters and data collected status collector marks the status of the device, and the RDSM–EBGWO controller uses this information to shift and schedule the devices optimally.

2.2. User Comfort Loads (UCLs)

The main motive of the proposed RDSM approach is to reduce the peak demand, thereby minimizing the electricity consumption cost. At the same time, the user's comfort is also important for certain load types. The loads, such as ceiling fans, DC fans, LED lamps, compressors, and pure water pumps, are considered user comfort loads. The shifting and scheduling of these loads increase the user's dissatisfaction level. To increase the comfort level of these load types, solar PV generation (SPV) is associated with the proposed RDSM architecture. A 30 kW SPV was set up in the institutional premises that supply the user comfort loads, thus considerably decreasing the power consumed from the utility. This approach increases the user's satisfaction level by increasing the user comfort index (UCI), which indicates the satisfaction level of users for the particular load type.
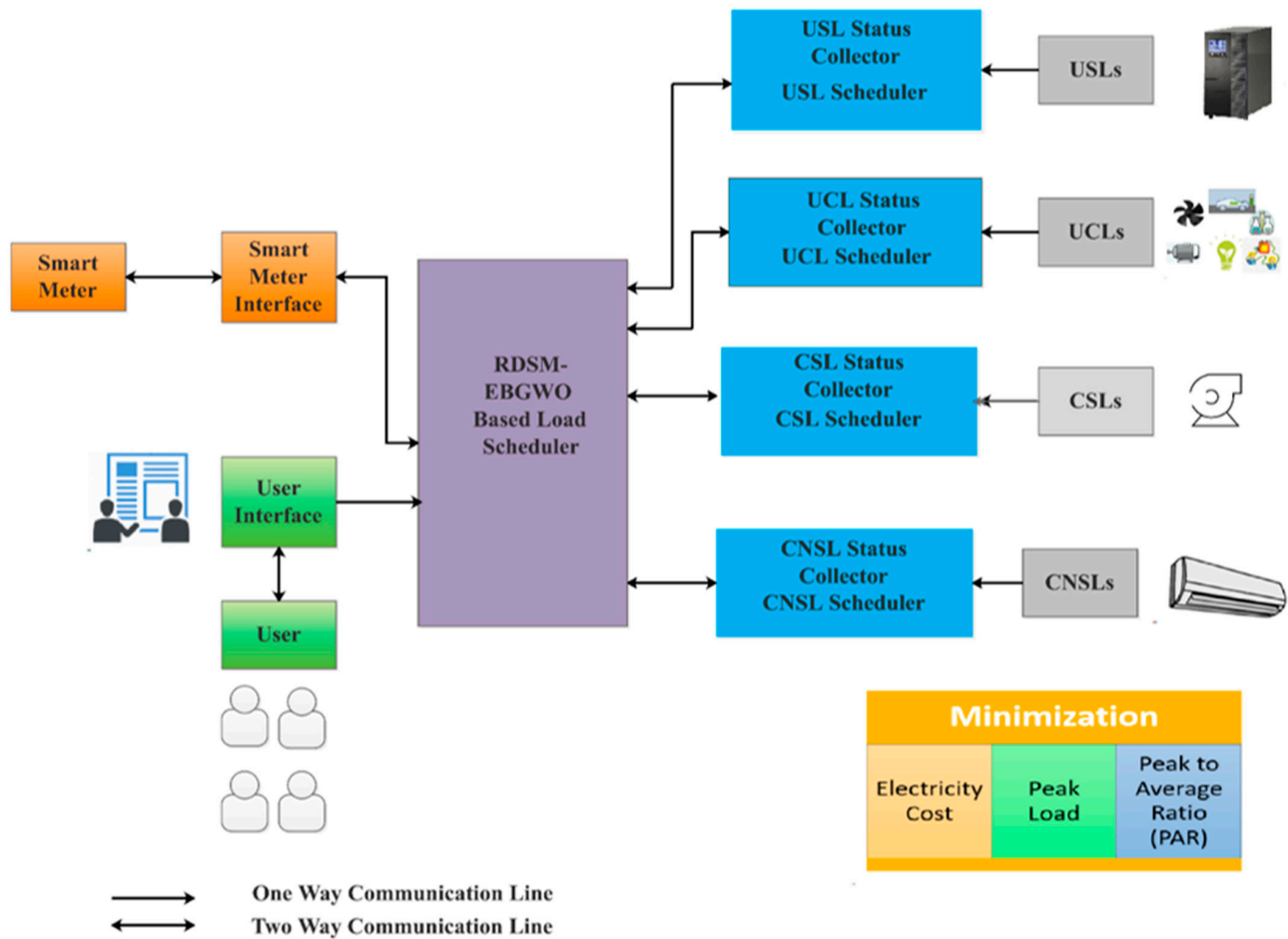
Figure 2. Architecture of the proposed RDSM–EBGWO.

3. Models of Load

The institutional demand data of KCET was considered for the analysis in this work. The loads are categorized into four major classes: uncontrollable non-shiftable loads (UNSLs), controllable non-shiftable loads (CNSLs), uncontrollable shiftable loads (USLs), and controllable shiftable loads (CSLs) along with SPV generation and plug-in electric vehicles (PHEVs). The institutional loads with load type and load name are enlisted in Appendix A. The various loads are classified and shown in Figure 3. The load types, Ideal working time with the start time (st) and end time (et), the effective period of operation, classification of load, power consumption and their category of either controlled or uncontrolled is tabulated in Table 1.

3.1. Modeling the UNSLs

The operating pattern of these user-controlled loads purely depends on the ON/OFF switching of the user at a given time in a day. The architecture model proposed sums up the demand for this type of load in an hour and ensures the demand does not exceed the sanctioned hourly demand. Let A represents the collection of UNSLs loads. The status vector represents the ON/OFF position of an UNSLs a ($a \in A = [1,2,3, \ldots ,A]$) in every interval ($i \in I = [1,2, \ldots .,24]$) is mentioned as:

$$Y_a = \left[y_a^1, y_a^2, \ldots \ldots \ldots , y_a^i, \ldots , y_a^{24} \right] \forall a \in A \tag{1}$$

Here A represents the total number of (UNSL) loads, and I represent the whole number of scheduling intervals on an entire day ($i = 24$).
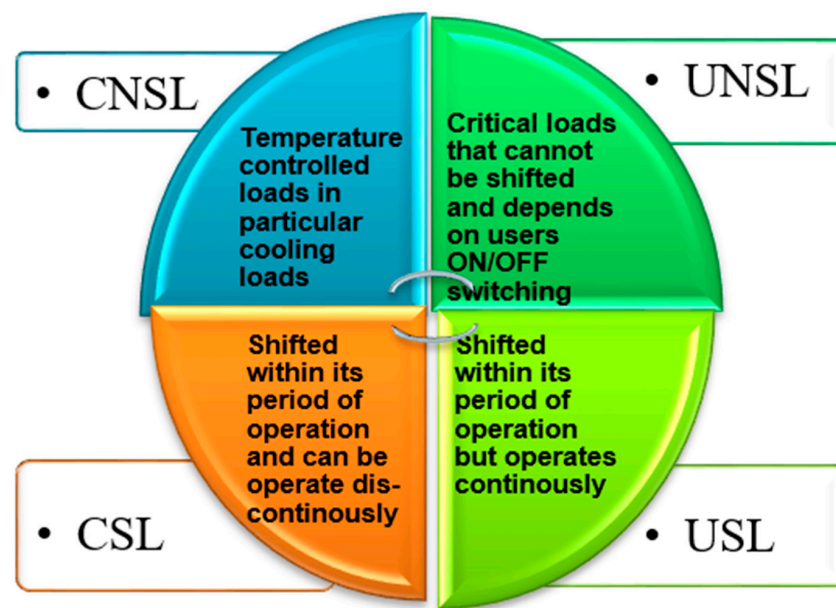
Figure 3. Classification of load types.

Table 1. Load types and their parameters specified.

Load Type	Ideal Working Time (st,et)	Period of Operation	Class	Power (kW)	Uncontrollable (U)/Controllable (C)
1	(9,16)	5	1	0.055	U
2	(8,16)	6	4	0.055	C
3	(10,17)	3	4	287.09	C
4	(1,23)	12	4	0.013	C
5	(9,20)	6	4	2.5	C
6	(9,16)	5	2	7.45	C
7	(9,16)	5	2	0.003	C
8	(8,16)	2	1	3.5	U
9	(1,23)	12	1	7.5	U
10	(9,16)	6	1	5.5	U
11	(5,10)	4	4	1.5	C
12	(5,10)	3	4	2.2	C
13	(6,10)	2	4	3.7	C
14	(8,17)	6	4	96.42	C
15	(9,16)	3	4	120.8	C
16	(9,16)	4	4	38	C
17	(9,16)	5	4	39	C
18	(9,16)	5	4	3.27	C
19	(9,16)	3	4	64.7	C
20	(9,16)	5	4	28	C
21	(9,16)	5	4	37	C
22	(9,16)	6	4	13	C
23	(9,16)	4	4	32.9	C
24	(9,16)	3	4	17.4	C
25	(9,16)	5	4	51.06	C
26	(9,16)	5	4	39.9	C
27	(9,16)	2	4	39	C
28	(9,16)	5	4	103.99	C
29	(9,16)	5	4	0.5	C
30	(8,15)	1	4	2.5	C
31	(9,16)	1	3	2.5	U
32	(9,16)	2	4	2.5	C
33	(9,16)	1	4	2.5	C
34	(9,16)	1	4	2.5	C

3.2. Model of CNSLs

The operating pattern of this type of load is temperature-dependent. These types of loads consume high power when in operation and less power when in STANDBY mode. In this paper, the cooling load is modeled by taking the frequency of the ON/OFF cycle of the air conditioner (ACs) into consideration. In other words, the frequency of the cycle for an hour of AC operation is counted for the efficient behavior of the device.

Let A denote the set of CNSLs, and I denote the set of monitoring intervals of non-shiftable loads (UNSLs and CNSLs). The operating vector representing the ON/OFF status of an CNSLs b ($b \in B \Delta = [1, 2, ..., B]$) in each interval i ($i \in I \Delta = [1, 2, ..., I]$) is defined as:

$$Y_b = \left[y_b^1, y_b^2, \ldots\ldots\ldots, y_b^i, \ldots, y_b^{24} \right] \forall b \in B \tag{2}$$

where I is the total number of non-shiftable load intervals in a day. Given the setpoint temperature, allowable tolerance limit, and frequency of cycle of operation of CNSL b as t_{set}^b, t_{tol}^b and $Cycle_b^i$, respectively. The actual temperature at the end of the interval $(i-1)$ as $t(i-1)_{act}^b$ the desired operating status of b during the interval i can be described as follows:

$$Y_b^i = \left\{ \begin{array}{c} 1, \ if \ t_{set}^b > (t_{set}^b + t_{tol}^b) \ And \ (Cycle_b^t == 4) \\ 0, \ if \ (t(i)_{act}^b < t_{set}^b) \ And \ ((Cycle_b^i > 4) \ Or \ (Cycle_b^i < 4)) \\ Y_b^{(i-1)}, \ if \ t_{set}^b \leq t(i)_{act}^b \leq (t_{set}^b + t_{tol}^b) \end{array} \right\} \tag{3}$$

The ON/OFF switching cycle frequency for cooling is once per 15 min of operation. Thus, in an hour, the cycle frequency for a normal operating cooling load is 4. The device malfunctions or consumes more power below or above this limit. However, the frequency of the cycle of operation differs with some models of ACs.

3.3. Model of SLs

The loads, which have higher feasibility of shifting in operation time, are modeling in this category. These are schedulable loads, which hardly rely on user comfort. There is high freedom in shifting these types of loads so that the peak load can be reduced, and cost savings can be increased considerably. The shiftable loads are further classified as uncontrollable shiftable loads (USLs) and controllable shiftable loads (CSLs).

3.3.1. Model of USLs

Schedulable loads that can only be operated continuously within their period of operation are categorized as uncontrollable shiftable loads. Let C represents the set of uninterruptible loads. The status vector represents the ON/OFF position of a USLs c ($c \in C = [1,2, \ldots ,C]$) on every interval is ($i \in I = [1,2, \ldots .,24]$) mentioned as:

$$Y_c = \left[y_c^1, y_c^2, \ldots\ldots., y_c^i, \ldots, y_c^{24} \right] \forall c \in C \tag{4}$$

where C is the total number of uncontrollable loads. These loads can be operated continuously within the start time (*st*) and the end time (*et*) to satisfy the load operating period. The operation status of USLs load c for interval i is mentioned as:

$$y_c^i = \left\{ \begin{array}{c} 0, \ i < st_c \ and \ i > et_c \\ 1, \ st_c \leq i \leq et_c \ and \ n_c^i \leq d_c \\ and [st_c : et_c] = d_c \end{array} \right. \tag{5}$$

where

st_c = start time for load c;

et_c = end time for load c;

st_c:etc = operating range from the start time to the end time;

$n_c{}^i$ = total number of load c operating hours to ith interval;
d_c = load c operating duration (in the total number of hours).

3.3.2. Model of CSLs

Loads that are schedulable but can be operated discontinuously within their period of operation in slots are categorized as controllable shiftable loads. Let D represents the controllable shiftable loads. The status vector represents the ON/OFF position of CSLs d ($d \in D = [1,2,3, \ldots ,D]$) in every interval ($i \in I = [1,2,3, \ldots .,24]$) is defined as:

$$Y_d = \left[y_d^1, y_d^2, \ldots\ldots\ldots, y_d^i, \ldots, y_d^{24} \right] \forall d \in D \tag{6}$$

where D is the number of controllable loads. These loads can be operated intermittently within the start time (st) and end time (et) for satisfying the load operating duration. The operating position of a CSL load d for interval i is:

$$y_d{}^i = \begin{cases} 0, & i < st_d \text{ and } i > et_d \\ 1, & st_d \leq i \leq et_d \text{ and } n_d{}^i \leq d_d \\ & and[st_d : et_d] = d_d \end{cases} \tag{7}$$

where

st_d = start time for load d;
et_d = end time for load d;
st_d, et_d = operating range from the start time to the end time;
$n_d{}^i$ = total number of load d operating hours to the ith interval;
d_d = load d operating duration (in the total number of hours).

4. Problem Formulation

A novel reinforced demand-side management (RDSM) technique was formulated for accomplishing the main objective of minimizing electricity cost and improving user comfort considerably. The problem formulated help in optimally shifting and scheduling the loads with the developed enhanced binary gray wolf optimization (EGBWO) algorithm for demand at the institutional load.

4.1. Objective Function

The leading objective of the proposed RDSM–EBGWO approach is to achieve minimum electricity cost by optimally shifting and scheduling the institution loads while also acknowledging the user's comfort. The nonlinearity and dynamic nature of the real-time electricity pricing and the demand variations of the loads make the objective function also a nonlinear function. The formulated objective function is stated in Equation (8):

$$Min : Cost = \sum_{i=1}^{24} \sum_{r=1}^{n} S_r(i) \times PD_r \times Rate(i) \tag{8}$$

where i represents the hour of operation, which varies from 1 to 24, i.e., 24 h of a day n is the total number of load types considered for modeling that varies from 1 to n. Further,

$S_r(i)$ = status of load r at the ith hour of operation, i.e., *ON is 1 or OFF is 0*;
PD_r = power demand for the rth load; and
$Rate(i)$ = electricity price at the ith hour of operation.

4.2. Constrains

4.2.1. Load Duration

All the shiftable and non-shiftable loads are scheduled for 24 h of a day to satisfy their load duration. The load duration is the period of operation that the device type is expected to operate:

$$\text{subject to } \sum_{i=1}^{24} \sum_{r=1}^{n} S_r(i) = d_r \tag{9}$$

where d_r = number of operating hours of load type "r".

4.2.2. Total Daily Load Demand

The demand for loads shifted and scheduled for 24 h per day should be equal to the total daily demand of loads before scheduling:

$$\text{subject to } \sum_{i=1}^{24} \sum_{r=1}^{n} D_1(i)_r = \sum_{i=1}^{24} \sum_{r=1}^{n} D_2(i)_r \tag{10}$$

where $D_1(i)_r$ is the total daily demand before shifting at the ith hour of rth type of load, $D_2(i)_r$ is the total daily demand after shifting at the ith hour of rth type of load.

4.2.3. Power Demand at Any Instant

The power demand by the user at any time must be near or equal to maximum power demand. This is shown in Equation (11):

$$PD_i \leq PD_{max} \ \forall \ i \in [1,24] \tag{11}$$

where PD_i = power demand at the ith hour of the day; PD_{max} = maximum power demand limit (MPDL) sanctioned.

The constraint is termed MPDL. It ensures that the maximum power demand does not exceed the programmed limit.

4.2.4. Idle Constraint

The devices should remain idle other than their operating period. This is referred to as idle constraint, as shown in Equation (12):

$$S_r(i) \ \forall \ i < st, i > et \text{ and } i \in [1,24] \ r \in [1,n] \tag{12}$$

$S_r(i)$ = status of load r at the ith hour of operation, i.e., ON is 1 or OFF is 0.

5. Optimization Algorithm

5.1. Binary Gray Wolf Optimization

Mirjalili et al. [25] created a new evolutionary algorithm known as gray wolf optimization (GWO) based on wolves' hunting behavior. In this algorithm, alpha (α) is considered as the *fittest* solution, beta (β) and delta (δ) are the second and third fittest solutions correspondingly. The remaining solutions are presumed as omega (ω). There are four different groups in the gray wolf pack: alpha, beta, delta, and omega. The alpha male makes decisions in hunting, selecting resting and sleeping places, etc. The rest of the family must obey its decisions. The dominant male alpha is placed at the top of the family pyramid. The mathematical model of the encircling behavior is presented in the following Equations (13) and (14):

$$\vec{D} = \left| \vec{C}.\vec{X}_p(t) - \vec{X}(t) \right| \tag{13}$$

$$\vec{X}(t+1) = \vec{X}_p(t) - \vec{A}.\vec{D} \tag{14}$$

where t is the current iteration, A and C are coefficient vectors, X_p is the position vector of the prey, and X indicates the position vector of a gray wolf. The coefficient vectors A and C are calculated using Equations (15) and (16) as follows:

$$\vec{A} = 2\vec{a}.\vec{r_1} - \vec{a} \tag{15}$$

$$\vec{C} = 2.\vec{r_2} \tag{16}$$

where components of "a" are linearly decreased from 2 to 0 throughout iterations, and r_1 and r_2 are random vectors in [0,1]. Emary et al. [26] introduced two methods for the binary version of GWO to choose the optimal feature subset for feature classification. In the first method, the updating equation of the particle position is framed as:

$$\vec{X}(t + 1) = Crossover\left(\vec{X_1}, \vec{X_2}, \vec{X_3}\right) \tag{17}$$

Crossover (x,y,z) is the suitable crossover between solutions x,y,z, and X_1, X_2, X_3. The binary vectors represent the movement of wolves towards alpha, beta, and delta gray wolves. In the second method, the updating equation of the particle position is mentioned as:

$$\vec{X}(t + 1) = \begin{cases} 1 \; if \; sigmoid\left(\dfrac{\vec{X_1} + \vec{X_2} + \vec{X_3}}{3}\right) \\ 0 \; otherwise \end{cases} \tag{18}$$

The initial population in the BGWO algorithm is set as 200, and the maximum number of iterations is 300. The algorithm is considered to be converged when the fitness value does not change in 50 iterations, and the alpha position is set as the best schedule in the final iteration. The BGWO algorithm's solution vector for each load type is a [1 × 24] vector:

$$P_{BGWO} = [s_1 \; s_2 \; s_3 \ldots\ldots\ldots\ldots\ldots s_{24}] \tag{19}$$

where P_{BGWO} = BGWO algorithm's solution vector;

S_k = load type "k" status = 1 (ON) or 0 (OFF).

Equation (19) shows the BGWO algorithm with the fitness function. It will return the bit vector for every load type with the optimized minimum cost.

5.2. Enhanced Binary Gray Wolf Optimization

Pei Hu et al. [32] proposed an enhanced binary gray wolf optimization (EBGWO), which is the improved version of the binary gray wolf algorithm (BGWO). The proposed EBGWO has the following enhancements:

- An improved "a" parameter is proposed, which plays a vital role in controlling the A and D influencing the exploration and exploitation;
- The proposed new transfer function and the updating equation for the "a" parameter balances the abilities of the global and local search of the algorithm.

The transfer function is the simplest method in the binary GWO, which maps the continuous values to [0,1] and then discretizes them to 0 and 1 according to the probability. BGWO uses the $S1$ transfer function as stated in Equation (20):

$$S1 = 1/(1 + e^{-10(A^d.D^d - 0.5)}) \tag{20}$$

BGWO is known to use $S1$ as the transfer function. The transfer function is a key part of the binary GWO and is an easy method to control the exploration and exploitation of the algorithm. Three new V-type transfer functions are introduced by Pei Hu proposed

to enhance the functionality of BGWO. Equations (21)–(23) give details for the *V* transfer functions. Equation (24) details the "*a*" parameter:

$$V1 \ = \ (x) \ | / tanh \ tanh \ (4) \tag{21}$$

$$V2 \ = \ |\sqrt{17} \ \times \ \frac{x}{(4 \ \times \ \sqrt{(1 \ + \ x^2)}|} \tag{22}$$

$$V3 \ = \ |\left(\frac{2}{\pi} \ x\right) / arctan(2\pi)| \tag{23}$$

$$a \ = \ 2 \ \times \ it / max\_it \tag{24}$$

where *it* = iteration and *max_it* = maximum iteration. In Equation (24), "*a*" increases linearly from 0 to 2. All three *V*-type transfer functions were deployed to the test system considered to find which transfer function gives optimal results.

6. Implementation

6.1. Proposed Methodology

The proposed reinforced demand-side management (RDSM) aids to optimally schedule loads by deploying the new enhanced binary gray wolf optimization algorithm (EBGWO). The loads are categorized into four classes, which have separate status collectors linked with the main RDSM–EBGWO controller. Initially, RDSM is fed with the details of the total load data of the institution and the real-time electricity pricing. The RDSM–EBGWO monitors and controls the load data based on the constraints stated in Section 4.2. Figure 4 details the flow of the proposed methodology.

6.2. Real-Time System

Demand-side management (DSM) is highly adopted by the consumer side, especially in the residential and institutional category of consumers. The proposed RDSM–EBGWO technique was implemented with the real-time system of KCET. In general, there are seven working hours for an educational institution, from 09:00 to 16:00. Within these 7 h, 09:00 to 12:00 is considered peak working hours in which real-time electricity pricing is also high. The main objective of the proposed methodology was to shift the loads from the peak hours to off-peak hours so that the electricity cost and peak demand will dwindle to a significant level. The electricity price in the peak hours, i.e., from 09:00 to 12:00, is higher than the off-peak hours. The peak pricing of USD 27.35/kWh at 10:00 and USD 8.11/kWh at 02:00 is the lowest in the off-peak hours.

6.3. User Input Data

The case study environment for the proposed methodology at KCET was initially studied without setting up the proposed RDSM–EBGWO techniques to perceive the peak demand and scheduling of the load. The input data were user-specified, and parameters like start time, end time, number of devices operated, period of operation and power (kW) are taken as input. As stated in Section 3, the category of classes was based on both periods of operation and the user's input. In this work, 34 different load types were considered, the use times and operation periods of which are tabulated in Table 2.
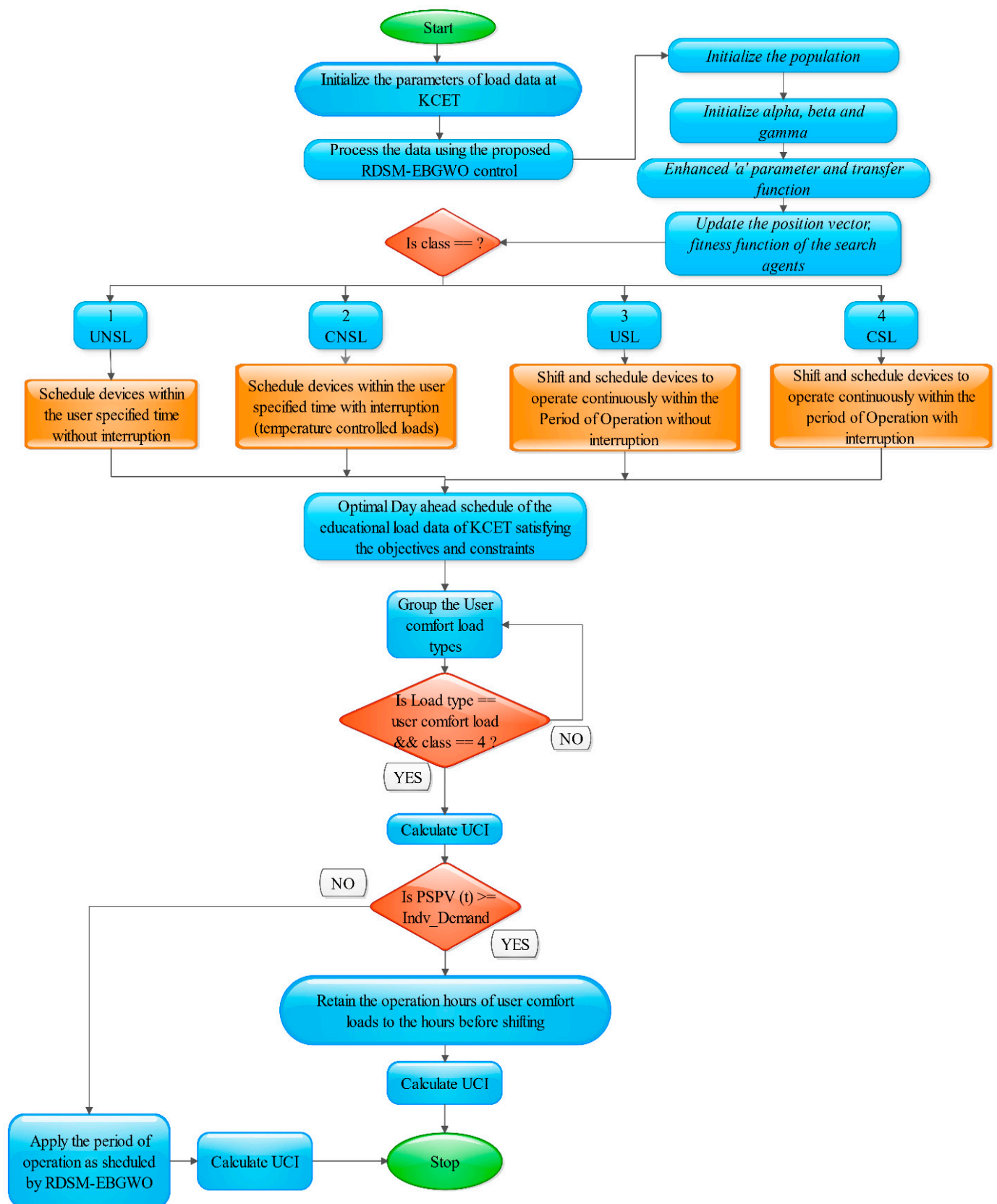
Figure 4. Flowchart of the proposed RDSM–EBGWO.

Load Type	Equipment	Period of Operation	Time of Use of Equipment
1	Ceiling fan 1	5	(9,10,11,12,13)
2	Ceiling fan 2	6	(9,10,12,13,14,16)
3	DC fan	3	(14,15,17)
4	Lights	12	(1,2,4,5,7,12,15,16,18,19,20,21)
5	LED lamps	6	(10,12,14,15,18,19)
6	1 phase AC	5	(11,12,13,14,15)
7	3 phase AC	5	(14,15,16,17,18)
8	Chargers	2	(6,7)
9	LAN communication	12	(8,9,10,11,12,13,14,15,16,17,18,19)
10	Elevator	6	(8,9,10,11,12,13)
11	Compressor 1	4	(5,6,8,10)
12	Sewage and water pumps	3	(7,9,10)
13	Compressor 2	2	(8,9)
14	Pure water pump	6	(8,11,12,14,15,16)
15	Polymer lab	3	(9,11,16)
16	Machine shop	4	(11,12,15,16)
17	Computer east load	5	(10,11,13,14,16)
18	Computer west load	5	(10,11,13,14,15)
19	Chemistry lab	3	(12,13,14)
20	Electrical lab	5	(9,10,12,14,15)
21	Mechanical lab	5	(9,10,11,15,16)
22	Admin	6	(9,11,12,13,14,15)
23	EIE	4	(12,13,14,15)
24	Polymer testing	3	(13,14,16)
25	ECE lab	5	(10,11,12,14,15)
26	Computer lab	5	(9,11,14,15,16)
27	Library lab	2	(10,13)
28	Biotech lab	5	(9,11,12,14,16)
29	IT lab	5	(10,11,13,14,16)
30	Invertors	1	14
31	PHEV charging1	1	9
32	PHEV charging 2	2	(10,11)
33	PHEV charging 3	1	11
34	PHEV charging 4	1	14

7. Results and Discussion

7.1. Demand without DSM

The study of the scheduling of loads without incorporating any DSM or DR techniques plays a vital role in wisely categorizing and shifting the critical and non-critical loads to accomplish the desired objective of cost minimization. The electricity cost at 10:00 was observed to be USD 26.82/kWh, which was marked as the peak electricity pricing. The demand at off-peak hours was lower without load scheduling, which aided in shifting the load demands from peak hours to off-peak hours, reducing the electricity cost.

7.2. Case 1—Implementation of the Proposed RDSM–EBGWO

For the real-time system considered, the peak demand was very high without the RDSM–EBGWO controller. The proposed RDSM–EBGWO control identified the CSL load types and shifted them optimally from peak hours to off-peak hours, thus reducing the peak demand from 1855.468 kW to 384.17 kW, which reduced the electricity consumption cost from **USD** 2030.67 to **USD** 1377.63. Consider a CSL load type 4 whose individual power demand was 287.09 kW. Without implementing RDSM strategy, this lighting load operated at (9,10,11,12,13,14,15,16,17,18,19,20) hours with 12 h being its period of operation. The RDSM–EBGWO controller shifted the load type 4 to (1,2,4,5,7,15,16,17,18,19,20,21).

Figure 5 shows the hourly demand of the four classes considered. The shifting of the load type 4 ensured that the proposed RDSM–EBGWO controller was capable of

identifying the CSL load types. The proposed control algorithm was also efficient in shifting and scheduling the load types in off-peak hours. The peak pricing hours from 09:00 to 13:00 were shifted to 01:00 to 07:00, thus reducing the electricity cost by **USD** 653.05.
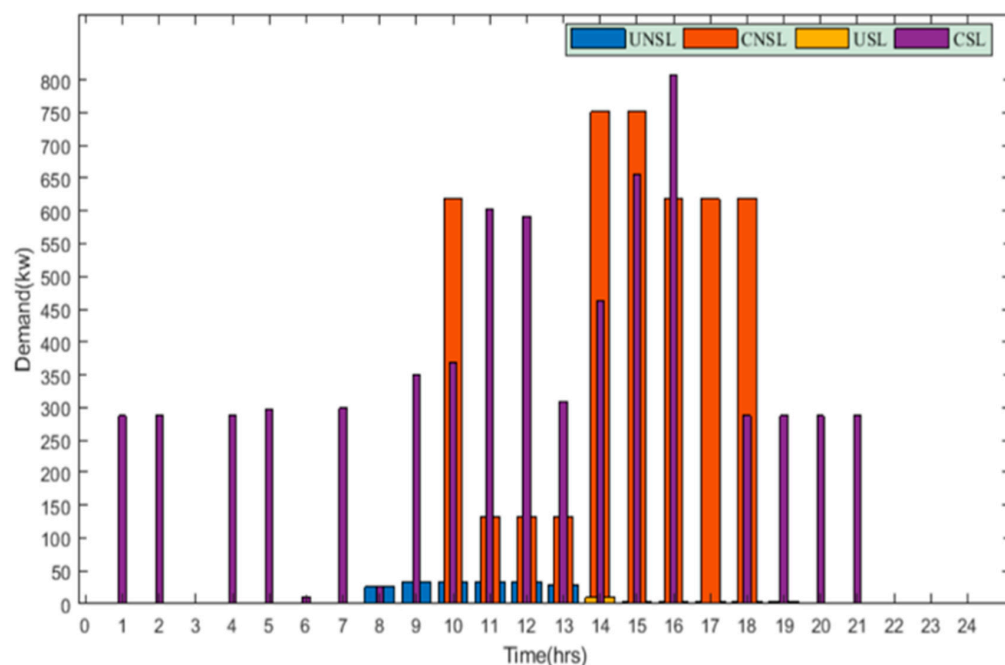

Figure 5. Hourly scheduling of loads based on the four categories of classes.

To test the optimality of the proposed EBGWO algorithm, two more swarm-based algorithms were deployed to the real-time system considered. They were binary particle swarm optimization (BPSO) and binary gray wolf algorithm (BGWO).

Table 3 shows various parameters of the PAR value and electricity cost after implementing the algorithm, and Table 4 details the obtained values of peak-to-average ratio (PAR), peak demand, electricity cost and its reduction with and without DSM. The reduction in PAR was 0.866 in BPSO, which was increased to 1.6989 after implementing EBGWO. The proposed RDSM–EBGWO had the highest cost savings of USD 653.046 compared to USD 612.396 and USD 562.99 that were the cost savings of BPSO and BGWO, respectively. Figure 6 shows the energy demand graph for before and after DSM with various optimization algorithms.

Table 3. PAR and cost values after implementing algorithms.

Criteria	BPSO			BGWO			EBGWO		
	Best	Mean	SD	Best	Mean	SD	Best	Mean	SD
PAR Value	3.263	3.2562	0.0073	2.7356	2.6477	0.0802	2.4297	2.4169	0.0109
Electricity Cost (USD)	1467.67	1488.76	8.627	1418.27	1436.22	6.91	1377.63	1382.46	3.99

Table 4. Comparison result for before and after implementation of algorithms.

| Criteria	BPSO			BGWO			EBGWO		
	Parameters			Parameters			Parameters		
	PAR	Peak Demand	Electricity Cost (USD)	PAR	Peak Demand	Electricity Cost (USD)	PAR	Peak Demand	Electricity Cost (USD)
Without DSM	4.129	1855.47	2030.67	4.1286	1855.47	2030.67	4.1286	1855.47	2030.67
With DSM	3.263	1502.238	1467.678	2.7356	1229.42	1418.27	2.4297	1091.97	1377.63
Reduction	0.866	353.23	562.9902	1.3930	626.0480	612.396	1.6989	763.4980	653.046
% Reduction	20.98	19.0372	27.7244	33.741	33.7407	30.1573	41.149	41.1485	32.1592
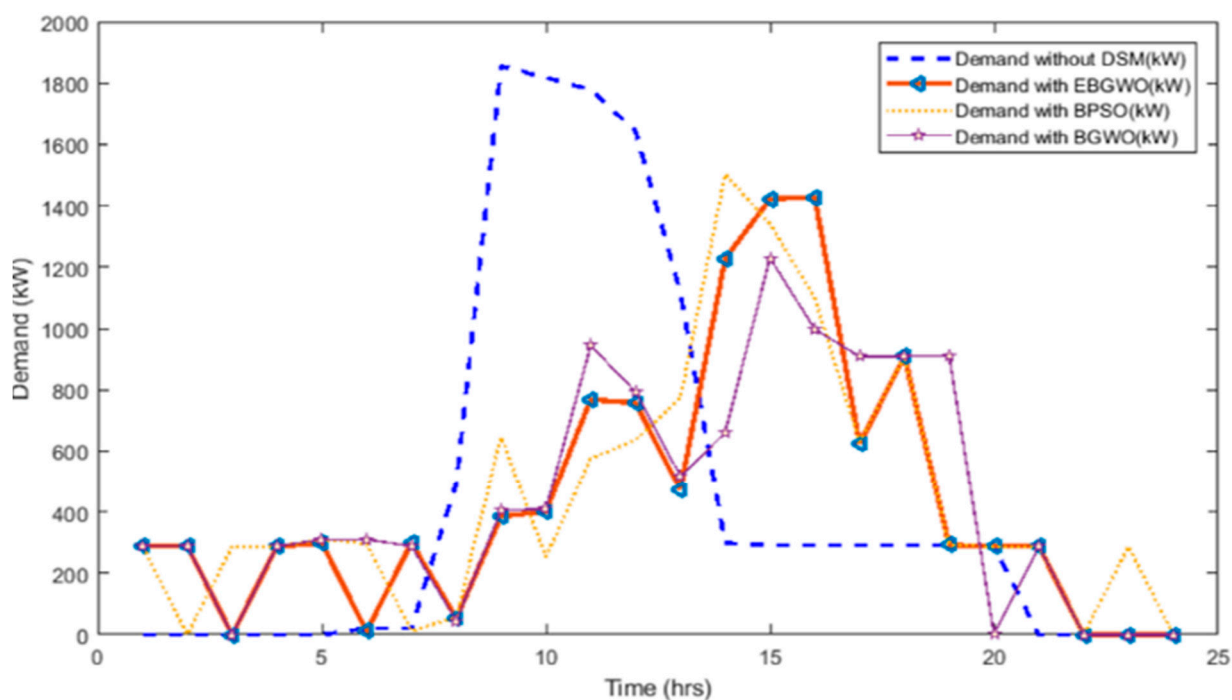
Figure 6. Demand before and after DSM with various optimization algorithms.

7.3. Case 2—Analysis of User Comfort Index (UCI)

The shifting of loads from the unscheduled time to the time slots after deploying optimization algorithms discomforts the user. Before deploying the RDSM–EBGWO based controller, the loads were scheduled to the user's preferences and comfort. The proposed controller shifted and scheduled these loads optimally to accomplish the objective of cost reduction. Even though the objective is reached, the comfort index of users decreased.

Table 5 details the period of operation both before and after deployment of the RDSM–EBGWO controller. The user comfort index (UCI) was obtained using the period of operation of the loads as in Equation (25):

$$\%UCI = \left(\frac{Number\ of\ Non-shifted\ hours\ of\ period\ of\ operation}{Total\ number\ of\ hours\ of\ the\ Period\ of\ operation} \right) \times 100 \qquad (25)$$

Table 5. Period of operation of user comfort loads before and after deployment of RDSM–EBGWO controller.

Load Type	Before Deploying RDSM–EBGWO Controller	After Deploying RDSM–EBGWO Controller	Number of Non-Shifted Hours of Period of Operation
2	(8,9,10,11,12,13)	(9,10,12,13,14,16)	4
3	(9,10,11)	(14,15,17)	0
5	(8,9,10,11,12,13)	(10,12,14,15,18,19)	2
11	(9,10,11,12)	(5,6,8,10)	1
13	(6,7)	(8,9)	0
14	(9,10,11,12,13,14)	(8,11,12,14,15,16)	3

The time of operation of each user comfort loads before and after scheduling is shown in Figures 7 and 8, respectively.
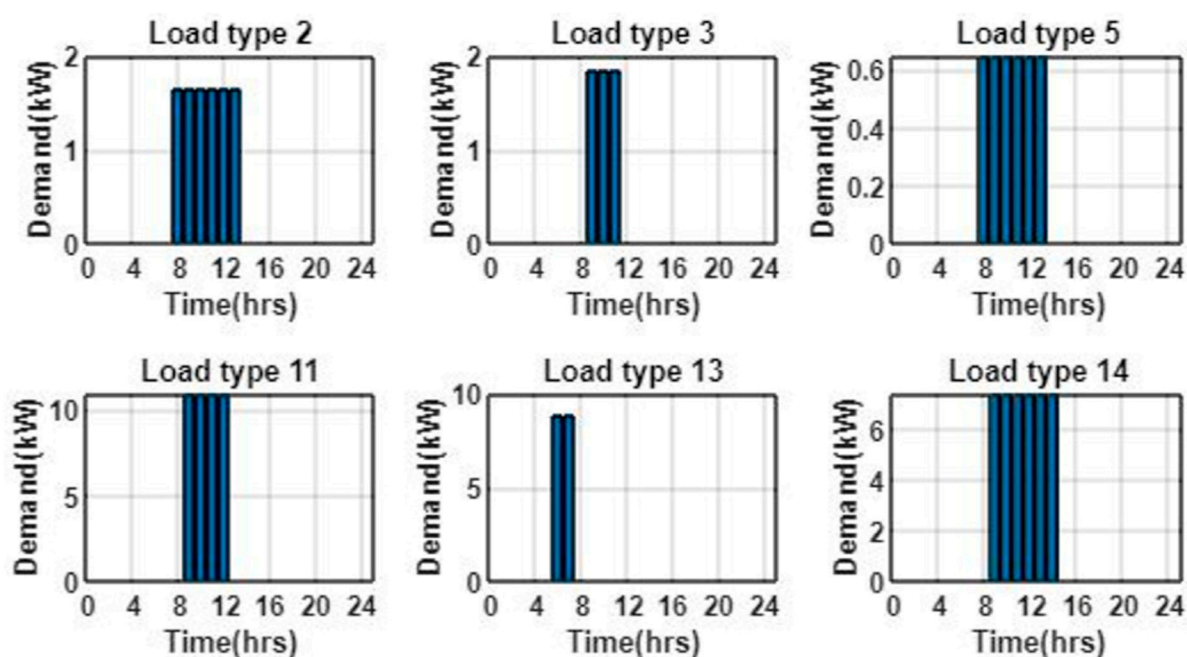
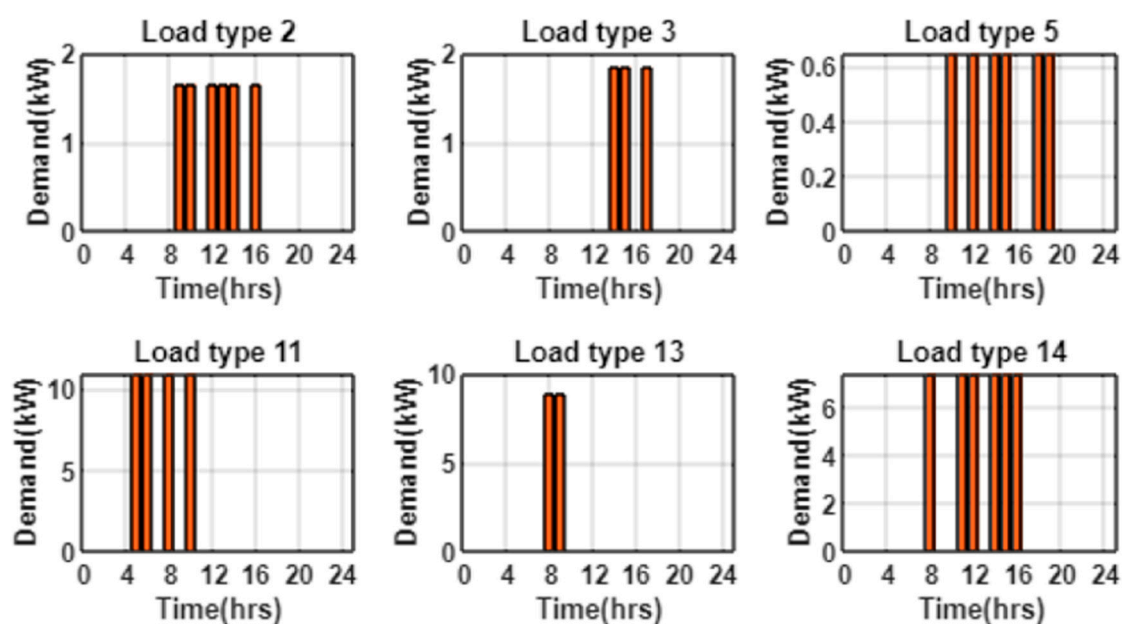**Figure 7.** Unscheduled operation of user comfort load before deployment of DSM.

Figure 8. Scheduled operation of user comfort load after deploying the proposed EBGWO.

Consider the load types: 3—DC fans and 13—compressors used in the college premises. The percentage of UCI of both loads 3 and 13 before deployment of the RDSM–EBGWO controller was 100% and was now reduced to 0%. This means that the period of operation of both the loads before deployment of the RDSM–EBGWO controller was completely different from that after deployment of the RDSM–EBGWO controller. This type of shifting of loads discomforted the users. The comfort was increased by retaining the period of operation as per users' desire. These loads were supplied by the solar PV instead of the utility supply so that this supports accomplishing the main objective of cost curtailment. After incorporating solar with these user comfort loads, the percentage of UCI of load types 3 and 13 were made 100% by retaining its period of operation as per user desire. Table 6 details the percent UCI of each load type considered as user comfort loads.

Table 6. User comfort index (UCI) before and after deployment of RDSM–EBGWO.

Load Type	Before Deployment of RDSM–EBGWO (%)	After Deployment of RDSM–EBGWO (%)	Increased Percentage of UCI Using Solar PV Generation (%)
2	100	66.7	33.3
3	100	0	100
5	100	33.3	66.7
11	100	25	75
13	100	0	100
14	100	50	50

The percentage of UCI of other load types 2,5,11, and 14 increased by 33.3%, 66.7%, 75%, and 50%, respectively. The individual demand for these loads was supplied by the 30 kW solar PV generation set up at KCET. The demand for the user comfort loads before and after RDSMEBGWO is shown in Figure 9. The demand at the eighth hour could be seen shifting from 2.7 kW to 27.2 kW, and this increase in demand was met by the SPV generation. It can be seen that the increase in UCI, as tabulated in Table 6, is clearly seen in demand increase at each hour in Figure 9.
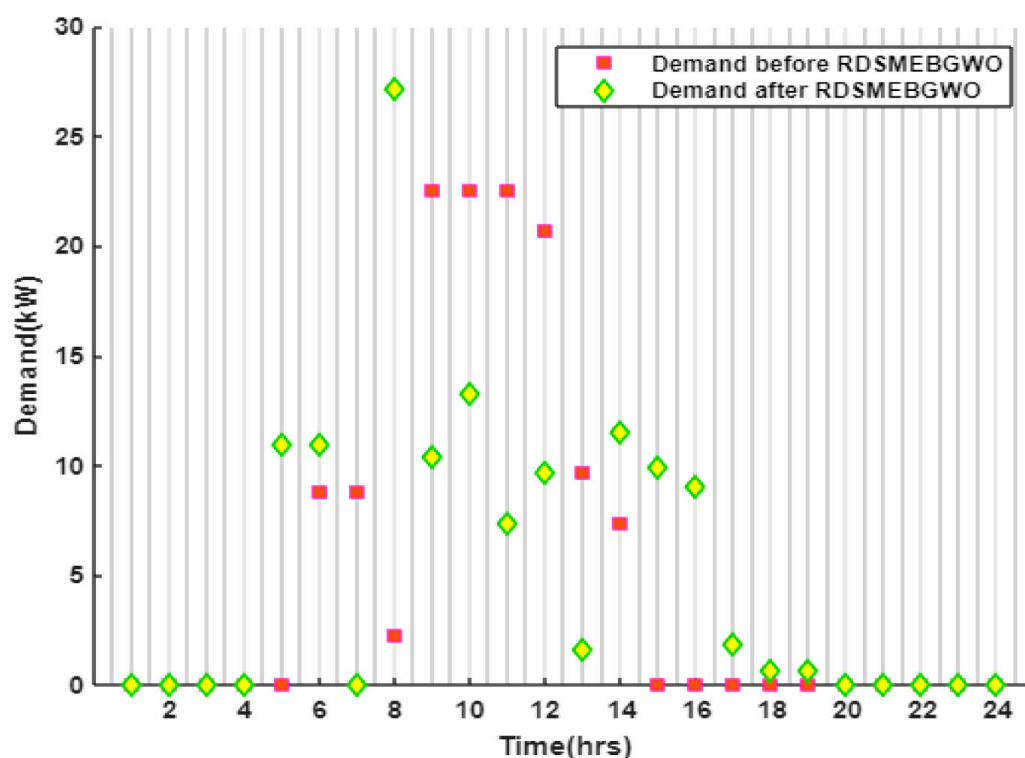
Figure 9. Demand for user comfort loads before and after RDSMEBGWO.

*7.4. Case 3—Temperature Controlled Class*

The class CNSL was modeled for temperature-controlled devices independently. The cooling load considered in this paper was commercial air conditioners (ACs). Tables 7 and 8 details the scheduling and shifting of AC loads and the parameters considered for modeling, respectively. It can be seen that both the single-phase and three-phase ACs were scheduled, neglecting the peak hours, i.e., 9:00 and 10:00, whose electricity pricing was high. As the study was conducted in an institution, the AC loads were shifted within the peak hours with lesser electricity pricing. The shifting of temperature-controlled load types 6 and 7 is detailed in Figure 10. The three-phase AC shifted from (9,10,11,12,13) hours of operation to (14,15,16,17,18) hours that had lesser electricity pricing. Because of this reason, the temperature-controlled load types were categorized under CNSL.

Table 7. Parameters for modeling temperature-dependent loads.

Load Type	Number of Devices	Ideal Working Time	Demand (kW)	Equipment	Shifted Hours of Operation
6	53	[9,16]	30	1-phase AC	[11,12,13,14,15]
7	83	[9,16]	35	3-phase AC	[14,15,16,17,18]

Table 8. Factors affecting the temperature-dependent load.

Setpoint Temperature	24.0 °C
Actual temperature	Instantaneous values of temperature within the period of operation of the equipment
Tolerance limit (ambient temperature, human ambulation)	0.05% of actual temperature
Cycle time	4 (Section 2)
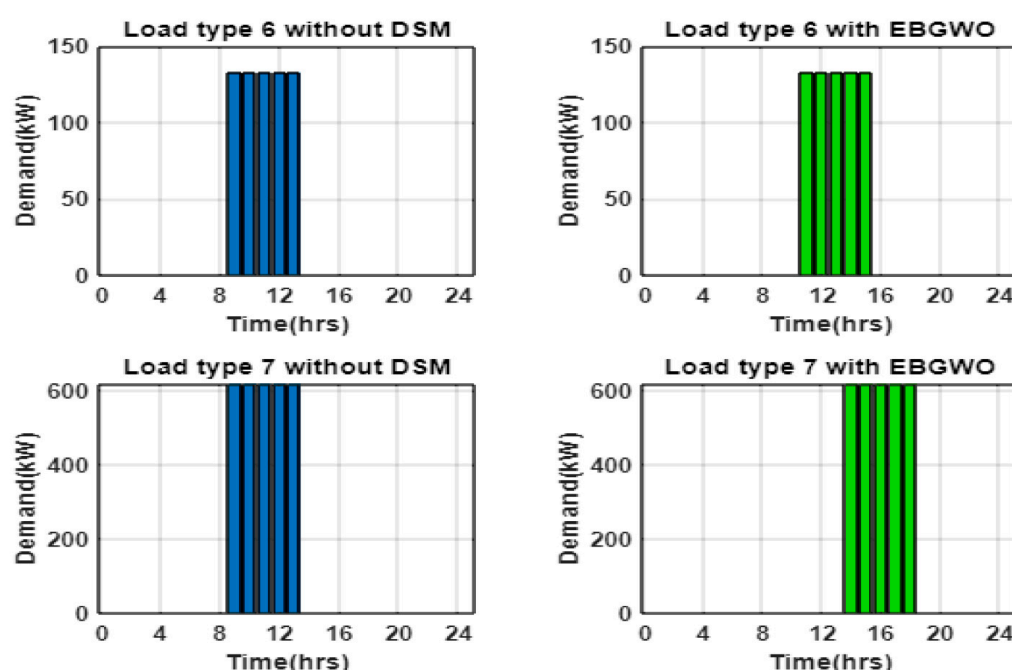
Figure 10. Shifting of load types 6 and 7 without DSM and with the proposed EBGWO.

8. Conclusions

The nonlinear objective function was effectively handled by the proposed RDSM–EBGWO algorithm, which was implemented in a real-time institutional load, accomplishing the following main objectives:

- Minimized electricity consumption cost.
- Significant reduction in PAR and peak demand.
- Shifted and scheduled the institutional loads optimally by considering the constraints.
- Modeled a separate class of loads for temperature-controlled air conditioners (AC).
- User comfort index (UCI) was introduced that helped to increase the user's satisfaction level for certain non-critical loads by incorporating the SPV.
- The percentage of electricity cost savings increased from 27.7244% to 32.1592% after deployment of BPSO and EBGWO, respectively.

Thus, the determined parameter values, such as peak demand, PAR and electricity cost, ensure that the proposed EBGWO gives the best results among other algorithms. Future work may include various pricing schemes, such as real-time pricing, time of use pricing and critical peak pricing. The DSM implemented with hybrid algorithms can also be developed.

Appendix A

Load Type	Number of Devices	Class	Load Name
1	128	1	Ceiling fan 1
2	30	4	Ceiling fan 2
3	48	4	DC fan
4	1	4	Lights
5	50	4	LED lamps
6	53	2	1 phase AC
7	83	2	3 phase AC
8	20	1	Chargers
9	1	1	LAN communication
10	3	1	Elevator
11	2	4	Compressor1
12	8	4	Sewage and water pumps
13	4	4	Compressor 2
14	2	4	Pure water pump
15	1	4	Polymer lab
16	1	4	Machine shop
17	1	4	Computer east load
18	1	4	Computer west load
19	1	4	Chemistry lab
20	1	4	Electrical lab
21	1	4	Mechanical lab
22	1	4	Admin
23	1	4	EIE
24	1	4	Polymer testing
25	1	4	ECE lab
26	1	4	Computer lab
27	1	4	Library lab
28	1	4	Biotech lab
29	1	4	IT lab
30	20	3	Invertors
31	5	4	PHEV charging 1
32	5	4	PHEV charging 2
33	5	4	PHEV charging 3
34	5	4	PHEV charging 4

References

1. Pedrasa, M.A.A.; Spooner, T.D.; MacGill, I.F. Scheduling of Demand Side Resources Using Binary Particle Swarm Optimization. *IEEE Trans. Power Syst.* **2009**, *24*, 1173–1181. [CrossRef]
2. Logenthiran, T.; Srinivasan, D.; Shun, T.Z. Demand Side Management in Smart Grid Using Heuristic Optimization. *IEEE Trans. Smart Grid* **2012**, *3*, 1244–1252. [CrossRef]
3. Logenthiran, T.; Srinivasan, D.; Phyu, E. Particle swarm optimization for demand side management in smart grid. In Proceedings of the 2015 IEEE Innovative Smart Grid Technologies—Asia (ISGT ASIA), Bangkok, Thailand, 3–6 November 2015; pp. 1–6.
4. Liu, E.; Cheng, P. Achieving Privacy Protection Using Distributed Load Scheduling: A Randomized Approach. *IEEE Trans. Smart Grid* **2017**, *8*, 2460–2473. [CrossRef]
5. Zakariazadeh, A.; Jadid, S.; Siano, P. Smart microgrid energy and reserve scheduling with demand response using stochastic optimization. *Electr. Power Energy Syst.* **2014**, *63*, 523–533. [CrossRef]
6. Arun, S.L.; Selvan, M.P. Intelligent Residential Energy Management System for Dynamic Demand Response in Smart Buildings. *IEEE Syst. J.* **2017**, *12*, 1329–1340. [CrossRef]
7. Bhamidi, L.; Sivasubramani, S. Optimal Planning and Operational Strategy of a Residential Microgrid With Demand Side Management. *IEEE Syst. J.* **2020**, *14*, 2624–2632. [CrossRef]
8. Park, L.; Jang, Y.; Cho, S.; Kim, J. Residential Demand Response for Renewable Energy Resources in Smart Grid Systems. *IEEE Trans. Ind. Inform.* **2017**, *13*, 3165–3173. [CrossRef]
9. Ravada, B.R.; Tummuru, N.R. Control of a Supercapacitor-Battery-PV Based Stand-Alone DC-Microgrid. *IEEE Trans. Energy Convers.* **2020**, *35*, 1268–1277. [CrossRef]
10. Mudaliyar, S.; Duggal, B.; Mishra, S. Distributed Tie-Line Power Flow Control of Autonomous DC Microgrid Clusters. *IEEE Trans. Power Electron.* **2020**, *35*, 11250–11266. [CrossRef]
11. Chaturvedi, S.; Fulwani, D.; Guerrero, J.M. Adaptive-SMC Based Output Impedance Shaping in DC Microgrids Affected by Inverter Loads. *IEEE Trans. Sustain. Energy* **2020**, *11*, 2940–2949. [CrossRef]
12. Hemanth, G.R.; Raja, S.C.; Nesamalar, J.J.D.; Kumar, J.S. Cost effective energy consumption in a residential building by implementing demand side management in the presence of different classes of power loads. *Adv. Build. Energy Res.* **2020**, 1–26. [CrossRef]
13. Chuan, L.; Ukil, A. Modeling and validation of electrical load profiling in residential buildings in Singapore. *2015 IEEE Power Energy Soc. Gen. Meet.* **2015**, *30*, 2800–2809. [CrossRef]
14. Arun, S.L.; Selvan, M.P. Dynamic demand response in smart buildings using an intelligent residential load management system. *IET Gener. Transm. Distrib.* **2017**, *11*, 4348–4357. [CrossRef]
15. Singh, S.; Namboodiri, A.; Selvan, M.P. Agent-based system to control the air-conditioner and EV charging for residents in smart cities. *IET Smart Cities* **2019**, *1*, 71–80. [CrossRef]
16. Qian, K.; Zhou, C.; Allan, M.; Yuan, Y. Modeling of Load DemandDue to EV Battery Charging in Distribution Systems. *IEEE Trans. Power Syst.* **2011**, *26*, 802–810. [CrossRef]
17. Lizondo, D.; Rodríguez, S.; Will, A.; Jimenez, V.; Gotay, J. An Artificial Immune Network for Distributed Demand-Side Management in Smart Grids. *Inf. Sci.* **2018**, *438*, 32–45. [CrossRef]
18. Zakariazadeh, A.; Jadid, S.; Siano, P. Economic-environmental energy and reserve scheduling of smart distribution systems: A multiobjective mathematical programming approach. *Energy Convers. Manag.* **2014**, *78*, 151–164. [CrossRef]
19. Qiu, J.; Meng, K.; Zheng, Y.; Dong, Z.Y. Optimal scheduling of distributed energy resources as a virtual power plant in a transactive energy framework. *IET Gener. Transm. Distrib.* **2017**, *11*, 3417–3427. [CrossRef]
20. Chen, Y.; Xu, P.; Chen, Z.; Wang, H.; Sha, H.; Ji, Y.; Zhang, Y.; Dou, Q.; Wang, S. Experimental investigation of demand response potential of buildings: Combined passive thermal mass and active storage. *Appl. Energy* **2020**, *280*, 115956. [CrossRef]
21. Nivethitha, S.; Gauthama Raman, M.R.; Ramamritham, K. A hybrid model for building energy consumption forecasting using long short term memory networks. *Appl. Energy* **2020**, *261*, 114131.
22. Yeo, J.; Wang, Y.; An, A.K.; Zhang, L. Estimation of energy efficiency for educational buildings in Hong Kong. *J. Clean. Prod.* **2019**, *235*, 453–460. [CrossRef]
23. Gui, X.; Gou, Z.; Zhang, F. The relationship between energy use and space use of higher educational buildings in subtropical Australia. *Energy Build.* **2020**, *211*, 109709. [CrossRef]
24. Shilpa, N.; Sridevi, H.R. Optimum design of Rooftop PV System for An Education Campus Using HOMER. In Proceedings of the 2019 Global Conference for Advancement in Technology (GCAT), Bangalore, India, 18–20 October 2019; pp. 1–4.
25. Basumatary, J.; Pratap Singh, B.; Gore, M.M. Demand Side Management of a University Load in Smart Grid Environment. In Proceedings of the Workshops co-located with the International Conference on Distributed Computing and Networks, Varanasi, India, 4–7 January 2018.
26. Helder, R.O.; Rocha, I.H.; Honorato, R.F.; Wanderley, C.; Celeste, L.J.; Silvestre, J.; Silva, A.L. An Artificial Intelligence based scheduling algorithm for demand-side energy management in Smart Homes. *Appl. Energy* **2021**, *282*, 116–145.
27. Mbungu, N.T.; Bansal, R.C.; Naidoo, R.M.; Bettayeb, M.; Siti, M.W.; Bipath, M. A dynamic energy management system using smart metering. *Appl. Energy* **2020**, *280*, 115990. [CrossRef]

28. Saffari, M.; de Gracia, A.; Fernández, C.; Belusko, M.; Boer, D.; Cabeza, L.F. Optimized demand side management (DSM) of peak electricity demand by coupling low temperature thermal energy storage (TES) and solar PV. *Appl. Energy* **2018**, *211*, 604–616. [CrossRef]

29. Mirjalili, S.; Mirjalili, S.M.; Lewis, A. Grey Wolf Optimizer. *Adv. Eng. Softw.* **2014**, *69*, 46–61. [CrossRef]

30. Tang, R.; Li, H.; Wang, S. A game theory-based decentralized control strategy for power demand management of building cluster using thermal mass and energy storage. *Appl. Energy* **2019**, *242*, 809–820. [CrossRef]

31. Emary, E.; Zawbaa, H.M.; Hassanien, A.E. Binary Gray Wolf Optimization Approaches for Feature Selection. *Neurocomputing* **2016**, *172*, 371–381. [CrossRef]

32. Hu, P.; Pan, J.-S.; Chu, S.-C. Improved Binary Grey Wolf Optimizer and Its application for feature selection. *Knowl. Based Syst.* **2020**, *195*, 105746. [CrossRef]

33. Rajvikram, M.E.; Leoponraj, S.; Vishnupriyan, J.; Dheeraj, A.; Gangaram, S. Multi-Criteria Decision Analysis for user satisfaction-induced demand-side load management for an institutional building. *Renew. Energy* **2021**, *170*, 1396–1426.

34. Rajvikram, M.E.; Leoponraj, S.; Vishnupriyan, J.; Dheeraj, A.; Gangaram, S.; Muhammad, I.; Mahesh, G.K. PV-Diesel-Hydrogen fuel cell based grid connected configurations for an institutional building using BWM framework and cost optimization algorithm. *Sustain. Energy Technol. Assess.* **2021**, *43*, 100934.

35. Nilotpal, C.; Arijit, M.; Samrat, M. Efficient Scheduling of Non-Preemptive Appliances for Peak Load Optimization in Smart Grid. *IEEE Trans. Ind. Inform.* **2017**, *8*, 3447–3458.

36. Ahmad, A.; Khan, J.Y. Real-Time Load Scheduling, Energy Storage Control and Comfort Management for Grid-Connected Solar Integrated Smart Buildings. *Appl. Energy* **2019**, *259*, 114208. [CrossRef]

37. Waseem, M.; Lin, Z.; Liu, S.; Sajjad, I.A.; Aziz, T. Optimal GWCSO-based home appliances scheduling for demand response considering end-users comfort. *Electr. Power Syst. Res.* **2020**, *187*, 106477. [CrossRef]

38. Naderi, E.; Pourakbari-Kasmaei, M.; Lehtonen, M. Transmission expansion planning integrated with wind farms: A review, comparative study, and a novel profound search approach. *Int. J. Electr. Power Energy Syst.* **2020**, *115*, 105460. [CrossRef]

39. Naderi, E.; Pourakbari-Kasmaei, M.; Cerna, F.V.; Lehtonen, M. A novel hybrid self-adaptive heuristic algorithm to handle single- and multi-objective optimal power flow problems. *Int. J. Electr. Power Energy Syst.* **2020**, *125*, 106492. [CrossRef]